24th COBEM - 2017

24th ABCM International Congress of Mechanical Engineering
December 3-8, 2017, Curitiba, PR, Brazil

COBEM-2017-1068
MODELING AND CONTROL OF A MACRO-MICRO SYSTEM USING INTERACTION CONTROLLERS

Gustavo Jose Giardini Lahr
Lucas Fideles Costa
Thiago Boaventura
Glauco Augusto de Paula Caurin
Mechanical Engineering Department, São Carlos School of Engineering, University of São Paulo
{gjgl.lahr, lfidelescosta}@gmail.com, tboaventura@usp.br, gcaurin@sc.usp.br

Abstract.*Macro-micro systems have many different implementations in robotics. It is especially important since it combines the characteristics of two different robots, reaching a new different configuration with a performance that would not be possible using the systems separately. However, the implementation of interaction controllers depends on the compliant behavior of the structures, sensors, tools and environment. This paper presents a macro-micro modeling and interaction controller implementation, using a Delta robot (micro) and a Kuka KR16 (macro). Both robots are controlled for stability. The Delta robot has significantly lower stiffness compared to the Kuka, leading to a different modeling from the usual impedance controller with industrial robots. Results are presented for compliance and impedance controllers, along one and two degrees-of-freedom. The architecture proposed is stable for interaction, where impedance control with higher damping factor presented an enhanced behavior.*

Keywords: *Robot Modeling, Macro-micro systems, Interaction controller*

1. INTRODUCTION

The macro-micro concept applied into robotics returns to studies conducted in the 1980s (Tilley and Jr., 1986; Sharon, 1988), which proposed the idea of connecting two robots with different characteristics to achieve better results when compared to the systems in an isolated configuration. With the development of electronics and computation, macro-micro systems have been implemented on robotics, from chromosomes manipulation (Feng *et al.*, 2012), surgery aid (Selmy *et al.*, 2017) to forklifts fine motion (Aref *et al.*, 2014). Several industrial tasks can also apply these systems, taking advantage on its dynamic behavior for tasks such as assembly and machining (Schneider *et al.*, 2014).

One of the advantages in using a macro-micro configuration is the ability to unify different characteristics between two different robots: it creates a new mechanism with more degrees of freedom and different dynamic behavior. The macro portion consists of a robot with large constructive dimensions which has a large work envelope, with lower positioning precision if compared to the micro portion. The last is characterized by having a smaller range but with higher speeds and better positioning accuracy than the macro portion. In terms of position control, the macro system position the whole system in the surroundings of the task, while the micro executes the fine motion. For interaction control, the micro system, due to lower inertia and higher damping interface, brings a new force control approach to the resulting system.

This work presents results with a macro-micro architecture consisting of a KR16 robot (macro) and a Delta robot (micro), implementing an interaction control in one and two directions. A one degree of freedom (DOF) model is proposed and simulated results are presented. Experiments of interaction control for one DOF were conducted with impedance and compliance controllers only for micro system movement. A conjugated movement is presented, with displacement of the macro in one direction and force control on the perpendicular direction with the micro system.

2. INTERACTION CONTROLLERS

Interaction controllers are used when mechanical interaction between robot and environment is needed. Instead of dealing the contact as a disturbance or a uncertainty, this class of controllers emulates a dynamical behavior for the manipulator which fits the application. In this way, transitions of control policies are not required, because switching between controllers may lead to instabilities.

There are two main classes: direct and indirect controllers. Direct is the name given to the techniques which control forces and torques through closing the loop with the measurement of the efforts themselves. Parallel (Chiaverini and Sci-

avicco, 1993) and hybrid (Raibert and Craig, 1981) controllers are examples of this category. On the other hand, indirect controllers modulate a relationship between flow (position and velocity) with effort (forces and torques). Compliance control (Mason, 1981) and impedance control (Hogan, 1985) are implementations examples of this class. Since it is not possible to actuate directly on the torques of industrial robots, due to its high reduction ratios and tuning of the position controller (Caccavale *et al.*, 2005), indirect interaction controllers are studied.

Impedance, at the mechanical domain, is a measure that correlates effort and flow. When it comes to industrial robots, efforts are forces and torques that may be measured using the force-torque sensors, while flow is given by displacement. Specifically for contact, the force measured is named interaction force ($F_{int}(s)$) and the displacement of the TCP is given by $X(s)$. Their relationship is given by Eq. (1), where the impedance parameters of interest are stiffness (K), damping (B), and inertia (M).

$$\frac{X}{F_{int}}(s) = \frac{1}{Ms^2 + Bs + K} \tag{1}$$

The same relationship between force and displacement applies for compliance control, with only the difference that it does not take into account high order derivatives, only the spring-like behavior. Thus, Eq. (2) displays the transfer function with the compliant term C, which is the inverse of the stiffness for linear systems, adopted in this study.

$$\frac{X}{F_{int}}(s) = \frac{1}{K} = C \tag{2}$$

Several effects may lead to instability during the interaction, such as environment stiffness, initial impact, non-collocated control, low damping interface and others (Eppinger and Seering, 1987).

3. MACRO-MICRO ARCHITECTURE

The first studies on macro-micro architectures argued that the industrial robots were not precise, responsive, or suitable to interact with the environment (Sharon *et al.*, 1993; Cho, 1997). These characteristics have changed a lot with the advancement of engineering. However, the dynamic concepts and the evaluation of the assembly of the systems are still valid for the control of these systems.

Sharon *et al.* (1993) point out that the position of the TCP is defined by reading the encoders of all joints, which can generate problems in certain applications where, for example, thermal expansion and mechanical deformation are not detected by the encoders. Add to this the problem that manipulators with large work envelopes need high torque motors to move all links and the load, so they lose in position accuracy and also the errors are carried from link to link until the TCP. And, despite all the improvements and changes that industrial robots have undergone, the best way to measure the forces in the tool is still to place the force sensor as close to the tool as possible. However, these robots have the actuators at the base of the links, resulting in a situation known as unplaced control, in which there is a dynamic between the sensor-actuator pair. This is problematic when high gains are needed (Eppinger and Seering, 1986).

Another complicating factor for the interaction controller is the initial impact, characterized by the sudden change of real speed and desired speed of the robot. The force generated by this interaction is read by the force sensor, however, in order for the controller calculation to take place and the control action to be performed on the actuator, some machine cycles have already occurred, generating a delay. This delay implies a post-impact performance and more values of path correction, which can generate instabilities. This feature is the source of a problem known as bounce or chatter, which is the effect of the robot losing contact with the surface (Love and Book, 1995), then returning to a stable position and strength, in more severe cases, the stabilized contact can never be reached. This problem can be alleviated by decreasing the TCP inertia, since velocity changes are defined by accelerations which are related to the inertia of the manipulator (Sharon *et al.*, 1993).

In this context, a micro system connected to a macro reduces this problem by providing a stable and adequate architecture for TCP control. Sharon *et al.* (1993) list three advantages of the macro-micro system in relation to the isolated systems. First, the regulation of the impedance of the tool center can be realized using the micro system, which increases the number of possible systems of interaction. Second, a micro system must be able to compensate for the accommodation time of a task, thus reducing cycle time. Third, the TCP inertia is physically reduced, which requires less effort by the actuators in the transient part of the contact, since the impact must first be felt by the micro system that has a lower inertia by definition.

Fig. 1a presents a serial manipulator (macro) connected to a parallel robot (micro) as an example of application. Fig. 1b presents a model of the proposed architecture: the macro manipulator is represented by joint dynamics equivalents, once the structural dynamics is detrimental in industrial robots (Sharon *et al.*, 1993), noted by M_1, B_1 and K_1; force transducer (M_2, K_2) and micro (M_1, B_1, K_1) are all represented, the interaction is presented as a interaction force, F_{int}. Each position along the DOF are noted by x.

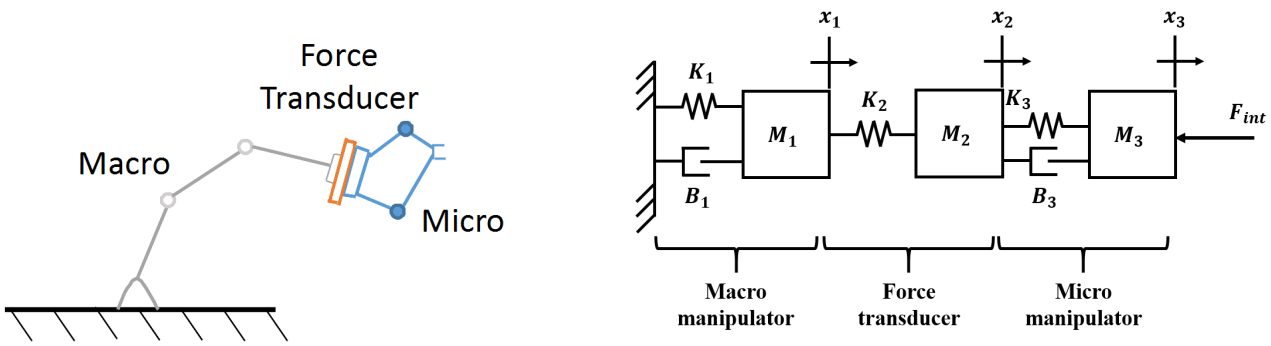

(a) Example of macro-micro system

(b) Model along one degree of freedom

Figure 1: Macro-micro modeling

Assuming a linear and time invariant model for Fig. 1b, it is possible to write the transfer function of the system, in respect with x_3 and the interaction force. Equation (3) is the respective transfer function, with the auxiliary equations noted by $\theta = M_1 s^2 + B_1 s + K_1 + K_2$, $\alpha = M_2 s^2 + B_3 s + K_2 + K_3$ and $\beta = M_3 s^2 + B_3 s + K_3$. These equations are related to each DOF.

Some numerical values are available or computed in accordance with the real values of the experimental setup used in this study. The force sensor parameters are defined by the manufacturer (ATI, 2016), as $M_2 = 0.93\ kg$ and $K_2 = 5.9 \times 10^7\ N/m$. For the macro robot, the parameters were adopted based on works with other robot models (Jubien *et al.*, 2014), which are $K_1 = 8.0 \times 10^7\ N/m$, $B_1 = 500\ Ns/m$ and $M_3 = 50\ kg$. Experimental verification will be conducted in future work, but the micro robot dynamics during interaction will experience low variation if changes are made to the macro's parameters, due to difference being orders of magnitude.

$$\frac{X_3}{F_{int}} = \frac{\theta\alpha^2 - K_2^2\alpha}{\beta(\theta\alpha^2 - K_2^2\alpha) - (B_3^2K_2^2s^2 + 2B_3K_2^2K_3s + K_2^2K_3^2)} \tag{3}$$

Figure 2 shows two Bode plots, which are related to the variation of the micro robot stiffness and damping parameters. The micro structure was measured with an scale, defining $M_3 = 0.64\ kg$, while K_3 and B_3 still open problems. Both parameters were simulated by varying from a specified range to evaluate the output and stability, with results shown at Fig. 2a for stiffness, and Fig. 2b for damping. All simulations presented a stable behavior for the linear case. Nonlinearities from change of unconstrained to constrained movement and stiffness of the environment are some causes that could lead to instability, which must be studied in future works.

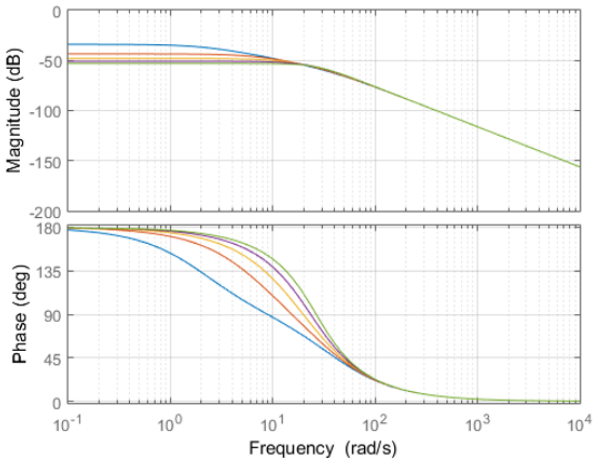

(a) Bode plot for the variation of delta robot stiffness: $50\ N/m \leq K_3 \leq 450\ N/m$ with damping maintained constant at $B_3 = 25\ Ns/m$. Maximum stiffness is displayed by the blue curve, while minimum is displayed by the green curve, all other values are intermediate.

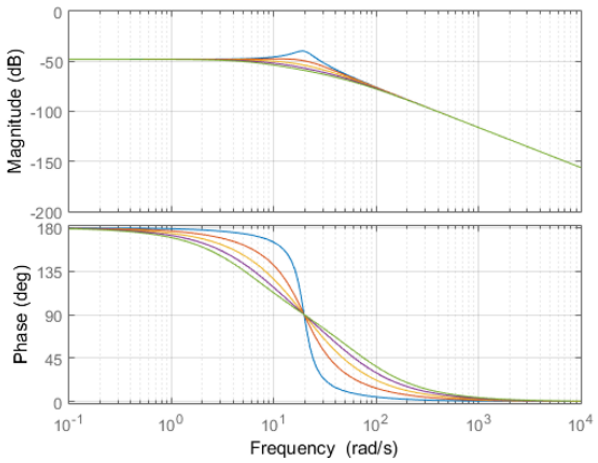

(b) Bode plot for the variation of delta robot damping: $10\ Ns/m \leq B_3 \leq 45\ Ns/m$. Stiffness constant at $K_3 = 250\ Ns/m$. The blue curve shows the system with the less damped system, i.e., $B_3 = 10\ Ns/m$, while the green curve shows the system with highest damping.

Figure 2: Bode plots for varying stiffness and damping for the delta robot

4. EXPERIMENTS

The macro-micro setup is shown by Fig. 3, where the force sensor (B) is placed between macro (A) and micro robots (C). The coordinate system of the delta robot is highlighted in the Fig. 3, and the blue Z axis is positive in the direction in which the delta robot distances itself from the base of the force sensor. The X (red) and Y (blue) axes form a plane parallel to the surface of the force sensor.

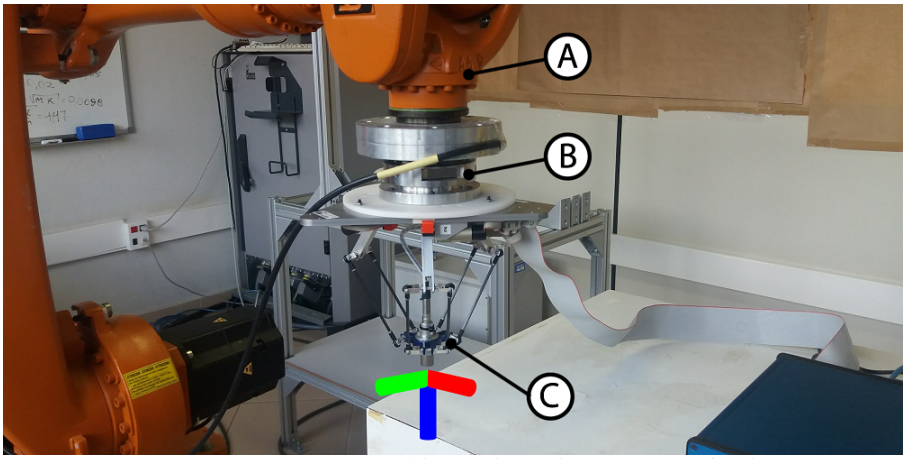

Figure 3: Experimental setup: (a) macro robot, a open kinematic chain Kuka KR16, with controller KR C2, maximum load of 16 kg and position accuracy of $\pm$ 0.05 mm and a work envelope of 1,611 m without tool. The RSI (Robot Sensor Interface) library version 2.3 is used to enable external communication using Ethernet UDP/IP protocol, with PC and the force torque sensor (b), from ATI Industrial Automation, model SI-660-60, which has a 1/8 N resolution on X and Y directions, and 1/4 N on Z direction. On (c) is the micro system, a closed chain delta robot, developed by the project EEROS. It has a maximum load of 0.5 kg and with a BeagleBone Black as controller, running with Linux as operational system.

Due to different hardware implementations, both systems have different time cycles. Kuka runs at a stable rate of 12 ms for each loop iteration, meanwhile, Delta is a robot in development, its loop varies between 15-19 ms. For this project, the loop was closed around the largest time step, creating a synchronous application with higher sampling time.

Two experiments were conducted to evaluate the assembly. Both experiments require the macro robot moving only on position control, with the micro only programmed with interaction control. The first experiment (Fig. 4a is a same direction movement with environment interaction, both moving on Z axis. For the second (Fig. 4b), Kuka moves on X direction and the Delta regulates the interaction in Z axis, where in its way is a bump-like shape along the way. In both the experiments, the desired force and position are zero.

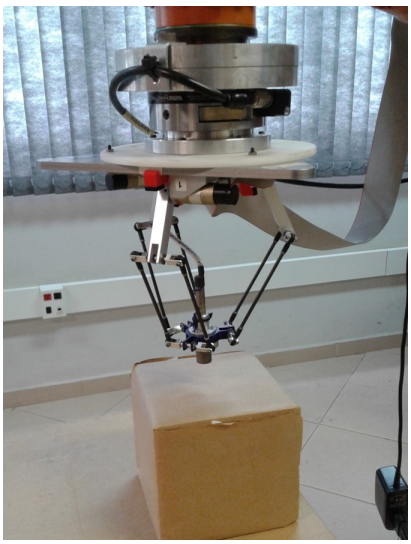

(a) Initial position

(b) Final position

Figure 4: Same direction experiment: the contact surface is soft, thus allowing better impedance matching. The micro system came into contact with a paperboard environment

4.1 Compliance control

Three different compliance controllers were tested for the same axis movement experiment, assuming a linear relationship for the stiffness-compliance pair, meaning that each compliance relates to a stiffness through its linear relationship (Eq. 2). The positions and forces are shown on Fig. 5.

It can be related that as the controller diminishes its compliance, the maximum force experienced increases. This is due the responsive behavior that is enhanced in highly compliant systems, when the compliance starts to decrease, the system becomes stiffer and, consequently, has a higher force. Also, indirect force controllers demand two inputs: desired position and force, which means, the delta was trying to control null force concomitantly with null displacement, i.e., it also was looking to remain at the same position. This indicates the existence of higher forces as the complacence lowers.

It can be defined as good performance a system with low oscillation and low contact forces, tending to an active compliant system. Controller C_3 presents, as the definition suggests, a poor performance system: it has a maximum contact force of 13.6 N, which is 10% higher than the controller C_2, with 12.2 N. Adding the facts that it is a situation with a nonlinear environment (soft) and the compliance controller just deals with zero-order parameters, i.e., displacement, active compliance for this situation is not suitable. C_1 presented small position changes, but the interaction force had a peak of 18.5 N, the highest between all three. As a mechanical interaction situation, controller C_2 had a better performance between over the other two candidates.

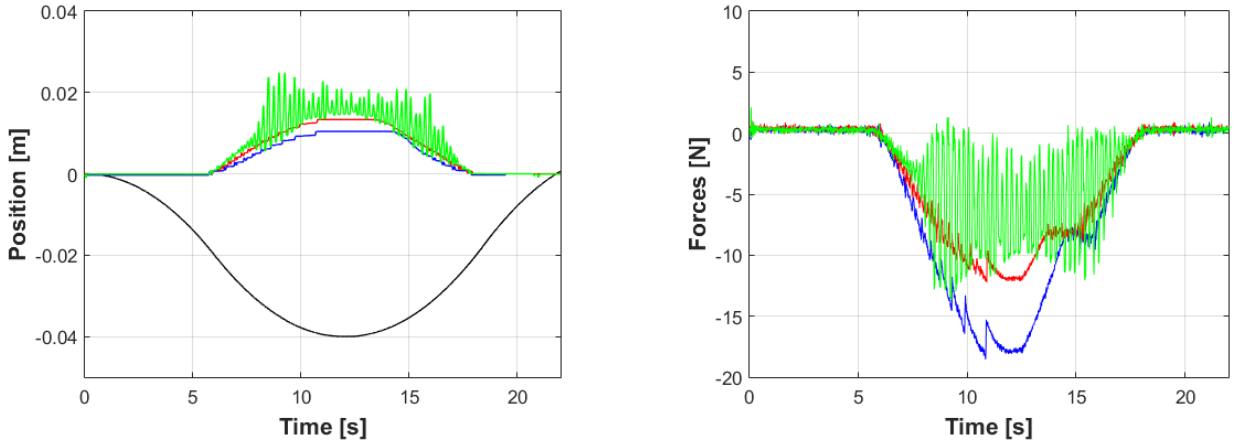

(a) Robot's positions where Kuka is the black line

(b) Interaction forces

Figure 5: Compliance control with Delta output: Blue - $C_1 = 0.5m/N$; Red - $C_2 = 1.0m/N$; Green - $C_3 = 2.0m/N$

4.2 Impedance Control

As the same experiment was conducted with impedance control, due to the amount of possible combinations, the following reasoning was applied: the chosen spring stiffness is the inverse of the used compliance; the mass value was chosen to be constant ($M = 0.004kg$); and the damping value was doubled once. The obtained results help to compare with the previous compliance, although we are aware that some practices may be applied to choose the best impedance parameters (Erickson *et al.*, 2003; Lahr *et al.*, 2017).

Six experiments are displayed at Fig. 6. The first group displays the micro robot relative position (Fig. 6a) and its respective forces (Fig. 6b) with damping coefficient of $\zeta = 0.35$. For its turn, the position and forces of the second group are shown by Fig. 6c and 6d, respectively, which are result from $\zeta = 0.7$. Table 1 shows the relationship about the time metrics and controller parameters, such as maximum force ($|F_{max}|$), maximum displacement ($|\Delta z_{max}|$), and presence or not of high frequency oscillations.

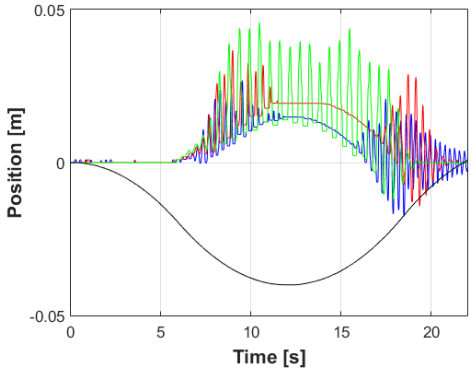

(a) Robot's positions - $\zeta = 0.35$ and Kuka as the black line

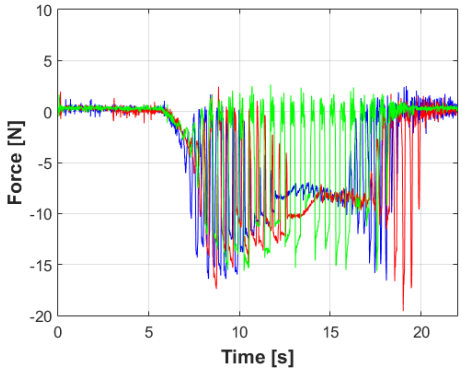

(b) Interaction forces - $\zeta = 0.35$

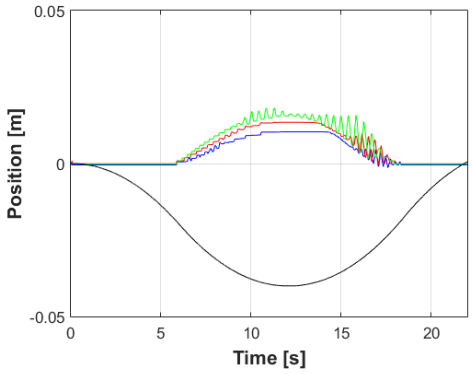

(c) Robot's positions - $\zeta = 0.70$ and Kuka as the black line

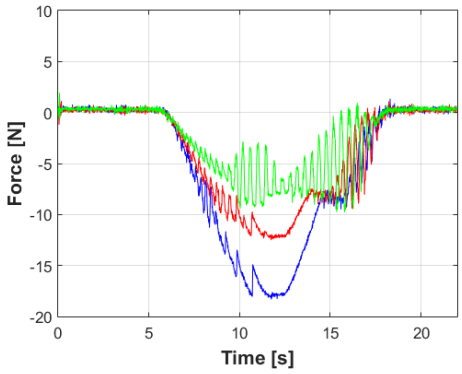

(d) Interaction forces - $\zeta = 0.70$

Figure 6: Impedance control: Blue - $K = 2.0\ N/m$; Red - $K = 1.0\ N/m$; Green - $K = 0.5\ N/m$

Fig. 6a presents high frequency oscillations, specially in approximation and return of the system. Fig. 6c shows the most interesting results, compared to the previous: although has three experiments with a factor of 2 at the stiffness differing each curve, all three present a maximum force very close to each other. This is related to the fact that the damping factor (ζ) was doubled, with a higher impact than stiffness. Small oscillations are presented, specially at the beginning and the end of the contact, which, in this case, stiffness tends to alleviate the oscillations.

In comparison with compliance controller results, the impedance approach presented more oscillations with higher amplitude for the experiment with lower damping factor. As the impedance controller presents more parameters, it allows a fine tuning of the characteristics of the task output, although it is harder to choose the best parameters.

Table 1: Impedance control parameters and time metrics

	Color	$B\ [Ns/m]$	$K\ [N/m]$	$\lvert F_{max}\rvert\ [N]$	$\lvert \Delta z_{max}\rvert\ [mm]$	Oscillations
$\zeta = 0.35$	Blue	0.06	2.0	16.6	26.8	yes
	Red	0.04	1.0	19.6	36.7	yes
	Green	0.03	0.5	15.7	45.8	yes
$\zeta = 0.7$	Blue	0.12	2.0	18.3	10.4	no
	Red	0.09	1.0	12.5	13.5	yes
	Green	0.06	0.5	9.7	18.0	no

4.3 Lateral movement

The lateral movement is defined by Kuka moving in the X-axis with only position control, the velocity was set to 25 mm/s, while the Delta robot corrects the interaction with impedance control on Z-axis. While the current macro system has a high mechanical stiffness, the micro has a low stiffness, which forced the experiment to have a soft environment for interaction. Otherwise, even controlling the interaction only in Z, the Delta robot experienced mechanical deformations in direction which was supposed to be maintained still. Fig. 7 presents the displacement and interaction forces (5.4 N for $\zeta = 0.35$ and 4.7 for ζ=0.7) for the experiment.

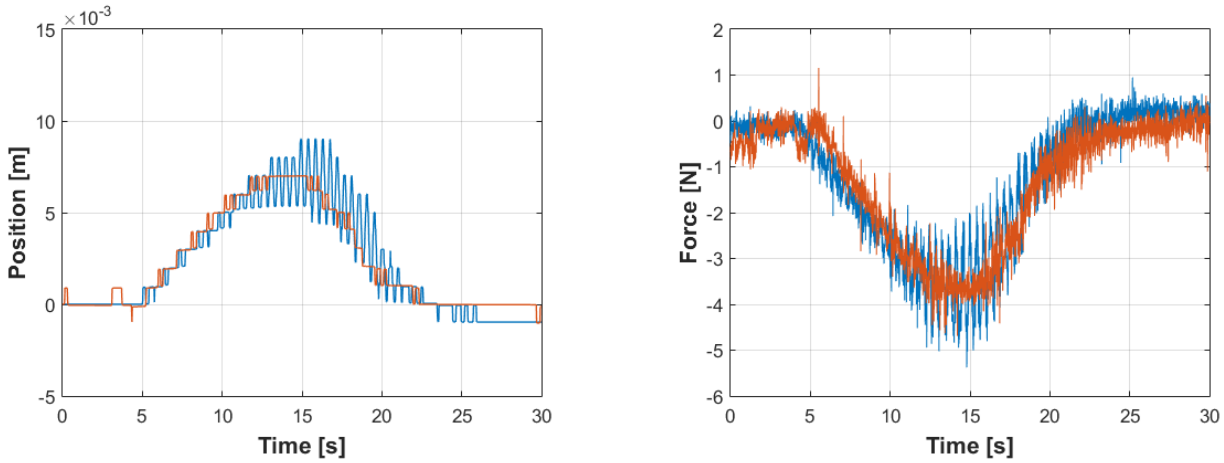

(a) Delta displacement in Z-axis with Red - $\zeta = 0.70$ and Blue - $\zeta = 0.35$

(b) Interaction forces

Figure 7: Outputs for impedance control during lateral movement

5. CONCLUSIONS

A macro-micro structure was proposed, consisting of an industrial open-chain manipulator as the macro robot, and a delta robot as the micro. This architecture is stable for well tuned compliance and impedance controllers, where both presented similar results. Impedance controller with low damping factor had the most oscillatory behavior and higher amplitude, while compliance control presented a satisfactory performance. Compared to only one parameter at compliance control, impedance is a strong candidate for future applications, once it deals with higher derivatives of flow (velocity and acceleration).

Future work includes the identification and simulation of the rigid body model of the coupled macro-micro system, as well as the investigation of interaction performance with stiff objects or environments. Furthermore, improvements in the control architecture of the delta robot will be performed in order to further enhance the interaction performance. Finally, more complex trajectory profiles and assembly tasks will also be tested.

6. ACKNOWLEDGEMENTS

We would like to acknowledge EMBRAER (cooperation project GSI-1168-15), CNPq and CAPES.

7. REFERENCES

Aref, M.M., Ghabcheloo, R. and Mattila, J., 2014. "A macro-micro controller for pallet picking by an articulated-frame-steering hydraulic mobile machine". In *2014 IEEE International Conference on Robotics and Automation (ICRA)*. IEEE, pp. 6816–6822. ISBN 978-1-4799-3685-4. doi:10.1109/ICRA.2014.6907865.

ATI, 2016. "F/T Sensor: Delta".

Caccavale, F., Natale, C., Siciliano, B. and Villani, L., 2005. "Integration for the next generation". *IEEE Robotics & Automation Magazine*, Vol. 12, No. 3, pp. 53–64. ISSN 1070-9932. doi:10.1109/MRA.2005.1511869.

Chiaverini, S. and Sciavicco, L., 1993. "The parallel approach to force/position control of robotic manipulators". *IEEE Transactions on Robotics and Automation*, Vol. 9, No. 4, pp. 361–373. ISSN 1042296X. doi:10.1109/70.246048.

Cho, W., 1997. "Control of a high precision macro-micro robotic manipulator system". *KSME International Journal*, Vol. 11, No. 1, pp. 29–44. ISSN 1738-494X. doi:10.1007/BF02945224.

Eppinger, S. and Seering, W., 1987. "Understanding bandwidth limitations in robot force control". In *Proceedings. 1987 IEEE International Conference on Robotics and Automation*. Institute of Electrical and Electronics Engineers, Vol. 4, pp. 904–909. doi:10.1109/ROBOT.1987.1087932.

Eppinger, S. and Seering, W., 1986. "On dynamic models of robot force control". *Proceedings. 1986 IEEE International Conference on Robotics and Automation*, Vol. 3, pp. 29–34. doi:10.1109/ROBOT.1986.1087723.

Erickson, D., Weber, M. and Sharf, I., 2003. "Contact Stiffness and Damping Estimation for Robotic Systems". *The International Journal of Robotics Research*, Vol. 22, No. 1, pp. 41–57. ISSN 0278-3649. doi: 10.1177/0278364903022001004.

Feng, J., Gao, F., Zhao, X., Yue, Y. and Liu, R., 2012. "A new macro-micro dual drive parallel robot for chromosome dissection". *Journal of Mechanical Science and Technology*, Vol. 26, No. 1, pp. 187–194. ISSN 1738-494X. doi:

10.1007/s12206-011-0917-7.

Hogan, N., 1985. "Impedance control: An approach to manipulation: Parts I-III". *Journal of Dynamic Systems, Measurement and Control, Transactions of the ASME*, Vol. 107, No. 1, pp. 1–7. ISSN 00220434.

Jubien, A., Abba, G. and Gautier, M., 2014. "Joint Stiffness Identification of a Heavy Kuka Robot with a Low-cost Clamped End-effector Procedure". In *Proceedings of the 11th International Conference on Informatics in Control, Automation and Robotics*. SCITEPRESS - Science and and Technology Publications, pp. 585–591. ISBN 978-989-758-039-0. doi:10.5220/0005115805850591.

Lahr, G.J.G., Garcia, H.B., Savazzi, J.O., Moretti, C.B., Aroca, R.V., Pedro, L.M., Barbosa, G.F. and Caurin, G.A.d.P., 2017. "Adjustable interaction control using genetic algorithm for enhanced coupled dynamics in tool-part contact". In *2017 IEEE/RSJ International Conference on Intelligent Robots and Systems (IROS 2017)*. IEEE Robotics and Automation Society, Vancouver.

Love, L. and Book, W., 1995. "Environment estimation for enhanced impedance control". *Proc. IEEE Int. Conf. on Robotics and Automation (ICRA)*, Vol. 2, No. 3, pp. 1854–1859. ISSN 1050-4729. doi:10.1109/ROBOT.1995.525537.

Mason, M.T., 1981. "Compliance and Force Control for Computer Controlled Manipulators". *IEEE Transactions on Systems, Man, and Cybernetics*, Vol. 11, No. 6, pp. 418–432. ISSN 0018-9472. doi:10.1109/TSMC.1981.4308708.

Raibert, M.H. and Craig, J.J., 1981. "Hybrid Position/Force Control of Manipulators". *Journal of Dynamic Systems, Measurement, and Control*, Vol. 103, No. 2, p. 126. ISSN 00220434. doi:10.1115/1.3139652.

Schneider, U., Olofsson, B., SoÂĺrnmo, O., Drust, M., Robertsson, A., Hägele, M. and Johansson, R., 2014. "Integrated approach to robotic machining with macro/micro-actuation". *Robotics and Computer-Integrated Manufacturing*, Vol. 30, No. 6, pp. 636–647. ISSN 07365845. doi:10.1016/j.rcim.2014.04.001.

Selmy, M., Fanni, M. and Mohamed, A.M., 2017. "Micro/macro-positioning control of a novel contactless active robotic joint using active magnetic bearing". In *Proceedings of the IEEE International Conference on Industrial Technology*. IEEE, pp. 671–676. ISBN 9781509053209. doi:10.1109/ICIT.2017.7915439.

Sharon, A., 1988. "The macro/micro manipulator : an improved architecture for robot control".

Sharon, A., Hogan, N. and Hardt, D.E., 1993. "The macro/micro manipulator: An improved architecture for robot control". *Robotics and Computer-Integrated Manufacturing*, Vol. 10, No. 3, pp. 209–222. ISSN 07365845. doi:10.1016/0736-5845(93)90056-P.

Tilley, S.W. and Jr., R.H.C., 1986. "End Point Position and Force Control of a Flexible Manipulator with a Quick Wrist". In *Proceedings of the AIAA Guidance, Navigation and Control Conference*. Williamsburg, VA, pp. 41–49.

8. RESPONSIBILITY NOTICE

The authors are the only responsible for the printed material included in this paper.